Iranian Journal of Physics Research, Vol. 23, No. 3, 2023
DOI: 10.47176/ijpr.23.3.81746

The role of the temperature anisotropy in the deuterium-tritium fuel ignition under the effect of relativistic shock waves

F Khodadadi Azadboni[*1], M Mahdavi[2], and A Khademlo[2]

1. Department of Physics Education, Farhangian University, P.O. Box 14665-889, Tehran, Iran
2. Department of Nuclear Physics, Faculty of Basic Sciences, University of Mazandaran, P.O. Box 47415-416, Babolsar, Iran

E-mail: F.khodadadi@cfu.ac.ir

(Received 31 August 2023 ; in final form 17 December 2023)

Abstract

This paper investigates the influence of temperature anisotropy on the ignition criterion of deuterium-tritium fuel in fast ignition fusion schemes that rely on short-pulse lasers-generated shock waves. The results show that increasing the temperature anisotropy parameter, $\beta = T_{\perp}/T_{\parallel}$, unexpectedly increases the fraction of alpha particles created and deposited into the ignition domain. For $\beta < 1$, the maximum confinement parameter remains below 4 g/cm^2, whereas for $\beta > 1$, it exceeds 4 g/cm^2. The fusion energy fraction, f_{α}, decreases throughout the laser pulse irradiation of the fuel (1 picosecond). A 100-fold increase in the temperature anisotropy parameter, β, leads to a 38% increase in the required plasma density times the hot spot dimension for fuel ignition. However, for β less than 1, the fusion energy fraction deposited decreases with time and reaches its minimum value of about 0.1 at the end of the laser pulse.

Keywords: deuterium-tritium fuel, fast ignition, ignition criterion, temperature anisotropy

1. Introduction

Inertial confinement fusion (ICF) is a fusion energy method that involves compressing and heating a small amount of fusion material at high temperatures using strong external forces. The objective is to achieve high compression of the fusion fuel to high densities for a short period of time [1-3]. To enable fusion reactions to occur in sufficient quantities, the plasma must be maintained at a high temperature for a sufficiently long duration. There are three concepts associated with the compression and heating methods for fusion fuel using high-intensity lasers, including direct drive and fast ignition (FI). Fast ignition is an alternative approach to traditional inertial confinement fusion that has been proposed for about three decades. In this method, the DT fuel is initially compressed to a high density, but the temperature remains below the ignition temperature. Then, a small amount of pre-compressed fuel is rapidly heated to the ignition temperature by a second heating beam, creating a hot spot [4-9]. This allows for higher energy gain and potentially greater flexibility and freedom in target design. The outer layer of the fuel target receives energy from an extreme-intensity laser or heavy ion beam [10-12]. Relativistic shock waves can significantly enhance the ignition of deuterium-tritium fuel by compressing and heating the fuel to high temperatures and densities, promoting fusion reactions**.** In the fast ignition scenario, temperature anisotropy plays a key role in energy transportation. When a high-power laser pulse (intensities>10^{12}w/cm^2) interacts with deuterium-tritium fuel, the plasma of the fuel is heated only in the velocity dimension along the wave propagation direction, leading to a temperature anisotropy of the electron distribution. This plasma exerts a high pressure on the surrounding material, leading to the formation of an intense shock wave and the temperature anisotropy moving into the interior of the fuel pellet. In high-intensity laser-plasma interaction, the electron beams are produced at the critical density surface by the ponderomotive force. The ponderomotive force creates the shock wave as an igniter for pre-compressed fuel in the framework of fast ignition. The ponderomotive force is associated with the intense electromagnetic fields of the laser and pushed out of the fuel. Instabilities can also be driven by anisotropy in the temperatures parallel and perpendicular to the magnetic field. Then a large magnetic field of the order of 10^8 G is generated. Instabilities arise in the presence of the temperature anisotropy or momentum space anisotropy. These are often placed in the class of streaming instability. The anisotropic distribution functions in the velocity space may drive unstable electromagnetic modes. For asymmetrical angular distribution function about the x-axis, a positive second anisotropic distribution function $T_x > T_{\perp}$ drives

unstable $K_{\perp}$ modes, whereas a negative second anisotropic distribution function $T_x<T_{\perp}$ drives unstable K_x modes. The Weibel electromagnetic instability takes place when the electron perpendicular temperature exceeds the parallel one ($T_{\perp}>T_{\parallel}$), which creates electromagnetic waves propagating along the magnetic field and restoring isotropy in phase space [11-15]. Weibel instability is ubiquitous in many environments in space and astrophysical plasmas and shows a wide variety of conditions [16-18]. The fire hose instability occurs when the parallel temperature is larger than the perpendicular temperature and when the parallel thermal pressure exceeds the magnetic pressure ($T_{\parallel}>T_{\perp}$) and produces waves propagating along the magnetic field, relaxing the distribution to a more isotropic temperature. Mirror instability happens when the perpendicular temperature is higher than the parallel temperature, producing electromagnetic waves propagating across the magnetic field lines and also relaxing the plasma to an isotropic distribution [19,20]. In studying the interaction of ultra-intense and ultra-short laser pulses with a plasma, these instabilities have been extensively investigated in connection e.g., with fast ignition schemes in inertial fusion where magnetic guiding of energetic particles might be advantageous [21-31]. The energy deposition of beams in fuel plasma and ignition conditions can be affected by these instabilities and temperature anisotropy. The effect of the temperature anisotropy in the confinement parameter value, fusion energy fraction has not been investigated yet and it can represent a significant advancement in the fusion research field. It is important to note that the specific implications of temperature anisotropy on the ignition condition for DT fuel depend on the magnitude and spatial distribution of the anisotropy, as well as the plasma parameters and confinement strategies employed in the fusion system. Further research is needed to comprehensively understand and quantify these implications. The purpose of the present work is to study the influence of the temperature anisotropy induced by shock waves on dissipation potentials and, more importantly, on the ignition condition for deuterium-tritium fuel.

2. Energy balance equation

The deuterium-tritium fuel is important in ICF because DT fuel has the largest cross-section at a relatively low temperature. At collision energies of 25-300 keV, it has a cross-section of 1-5 barns and releases energy of 17.6 MeV. It is mainly in the form of a pellet with a radius of around 400 microns, which contains an admixture of deuterium and tritium [12]. The DT fuel is the main fuel in ICF due to the high reaction rate at a relatively low temperature. When these two nuclei (hydrogen isotopes) are fused, an unstable nucleus consisting of two protons and three neutrons is formed in the process. The nuclear reaction $D+T \rightarrow \alpha(3.5\,MeV)+n(14.1\,MeV)$ results in the immediate decomposition of the nucleus into a neutron with an energy of 14.1 MeV and an alpha particle with an energy of 3.5 MeV. Here, alpha refers to a charged helium ion (^4_2He) and n refers to a neutron. In terms of energy, 1 MeV is equivalent to 1.6×10^{-13} J. Therefore, the energy of the neutron is approximately 2.26×10^{-12} J (14.1 MeV× 1.6×10^{-13} J/MeV) and the energy of the alpha particle is approximately 5.6×10^{-13} J (3.5 MeV ×1.6×10^{-13} J/MeV). The fusion energy in this reaction is defined as $E_f=E_{\alpha}+E_n$, where E_{α} is α particle energy usually deposited in part into the ignition domain and E_n is the neutron particle energy and practically not contained in the ignition volume under consideration. Net energy production, instead, can be achieved when the reaction partners form a plasma of sufficiently high temperature. In thermal equilibrium, the Coulomb collisions just redistribute the kinetic energy among the plasma particles, and fusion reactions will occur eventually after a sequence of collisions. Thermonuclear ignition and burn of plasma occurs when internal heating by fusion products exceeds all energy losses such that no further external heating is necessary to keep the plasma in the burning state. Ignition requires a certain temperature, depending on the fusion fuel and the relevant loss mechanisms. The hot-spot ignition condition for the fuel pellet can be determined by considering the power balance between fusion energy deposition and energy loss terms. The equation describing the ignition requirement is defined by

$$W_f - \sum W\left(losses\right) \geq 0, \tag{1}$$

where W_f is the ignition fusion power and W_{losses} is the power density losses. The power density losses include the energy loss by electron bremsstrahlung (W_B), the heat out flux by electron conduction (W_{he}), and the mechanical work (W_m). The ignition fusion power W_f [erg/s.cm^3] is given by[3]:

$$W_f\left[\frac{erg}{cm^3.s}\right] = n_D n_T <\sigma v>_{DT} Q_{\alpha}$$
$$\sim 8.07\times10^{40} <\sigma v>_{DT} \rho_{DT}^2, \tag{2}$$

where Q_{α}=3.5 MeV is the α-particle energy, n_D and n_T are the appropriate densities of particles deuterium and tritons, respectively and $<\sigma v>_{DT}$ is the Maxwellian-averaged reaction rate. The reactivity $<\sigma v>_{DT}$ in the domain of ion temperatures 1 keV$<T_i<$100 keV is [3]

$$\prec \sigma v \succ_{DT} (\frac{cm^3}{s}) =$$
$$6.4341\times10^{-14}\varsigma^{-5/6}(\frac{6.661}{T_i})^2 \tag{3}$$
$$\exp(-19.983(\frac{\varsigma}{T_i(keV)})^{1/3}),$$

where ζ is

$$\varsigma = 1+\frac{0.10675T_i^{\,3}-4.6064T_i^{\,2}-15.136T_i}{0.01366T_i^{\,3}+13.5T_i^{\,2}+75.189T_i+1000}. \tag{4}$$

The α-particles move along a nearly straight path and their velocity decreases according to $-\frac{v_{\alpha}}{2t_{\alpha e}}$. The velocity of the 3.5 MeV α-particle is about 1.29×10^9 cm/s. The effective temperatures in the perpendicular and parallel

direction with respect to the wave propagation are given by [21]:

$$T_{\perp} = \frac{m_e}{n_0}\int v_z^{\,2} f_0(v) d^3 v \,, \tag{5}$$

$$T_{\parallel} = \frac{m_e}{2n_0}\int v_x^{\,2} f_0(v) d^3 v \,, \tag{6}$$

where f_0 is the anisotropy of the distribution function. Temperature anisotropy is denoted by $\beta = T_{\perp}/T_{\parallel}$, the temperature of electron T_e is defined as $T_e = (T_{\perp})^{\frac{2}{3}}.(T_{\parallel})^{\frac{1}{3}}$. In that case, T_e can be written as $T_e = \beta^{\frac{2}{3}} T_{\parallel}$. The temperature of the electron and ion are not equal. The characteristic time for energy deposition in Reference [12] is defined by $t_{\alpha e} = \frac{42 T_e^{3/2}}{\rho \ln \Lambda_{\alpha e}}$. For $T_{\parallel} \neq T_{\perp}$, the characteristic time is defined by:

$$t_{\alpha e} = \frac{42 T_{\perp} T_{\parallel}^{1/2}}{\rho \ln \Lambda_{\alpha e}}\, ps, \tag{7}$$

where $\ln\Lambda_{\alpha e}$ is the Coulomb logarithm for collisions between α-particles and electrons. For $T_{\perp} \neq T_{\parallel}$, the Coulomb logarithm is given by[14]:

$$\ln \Lambda = \frac{3}{2\sqrt{\pi} Z e^3}\sqrt{\frac{k_B^{\,2} T_{\perp}^{\,2} T_{\parallel}}{n_e}} \,, \tag{8}$$

In fact, the α -fusion energy is not completely deposited into the igniter zone. So, the fraction of alpha particles that deposited energy inside the igniter domain can be estimated as follows [11]:

$$f_{\alpha} = \begin{cases} \frac{3}{2}x_{\alpha} - \frac{4}{5}x_{\alpha}^2 & x_{\alpha} < \frac{1}{2} \\ 1 - \frac{1}{4x_{\alpha}} + \frac{1}{160 x_{\alpha}^3} & x_{\alpha} \geq \frac{1}{2}, \end{cases} \tag{9}$$

where

$$x_{\alpha}(\tau) = \frac{R}{R_{\alpha}}, \tag{10}$$

The igniter dimension R in our model is taken to be

$$R = \left(\frac{u_s}{c} - \frac{u_p}{c}\right) c\tau_L \,, \tag{11}$$

where u_s and u_p are the shock wave velocity and the particle velocity accordingly, τ_L is the laser pulse duration that causes ignition and, c is the speed of light. The velocities u_s and u_p depend on the laser and the fuel parameters. The range of a 3.5 MeV α-particle in a homogeneous plasma is obtained as $R_{\alpha} = \int v_{\alpha} dt$. Therefore $R_{\alpha} = t_{\alpha e} v_{\alpha}$ for the DT fuel is approximated by [3]:

$$R_{\alpha}[cm] = \frac{1}{\kappa \rho_0}\left[\frac{1.5\times 10^{-2}\left(\beta^{\frac{2}{3}} T_{\parallel}(KeV)\right)^{\frac{5}{4}}}{1 + 8.2\times 10^{-3}\left(\beta^{\frac{2}{3}} T_{\parallel}(KeV)\right)^{\frac{5}{4}}}\right]. \tag{12}$$

The initial density of the pre-compressed fuel is ρ_0 and κ is the shock wave compression during the fast ignition process. The environment temperature is much less than that of the fuel plasma. Therefore, very steep gradients in temperature will exist between the fuel plasma and its environment that leads to driving heat out of the plasma. The losses due to electron conduction from the igniter domain for DT plasma are approximated by [3]:

$$W_{he}[\frac{erg}{cm^3.s}] = \frac{K_e \beta^{\frac{2}{3}} T_{\parallel}}{R^2} = \frac{3.11\times 10^{9}\left(\beta^{\frac{2}{3}} T_{\parallel}(eV)\right)^{\frac{7}{2}}}{R^2 \ln \Lambda} . \tag{13}$$

Ion thermal conduction can be neglected since electron conductivity is a factor of the order of $\sqrt{m_i / m_e}$ larger than ion conductivity, with m_e and m_i being, respectively, the electron mass and the average ion mass. In a plasma with a temperature of a few keV, it is possible for the charged particles to lose part of their energies through light emission during deceleration by plasma ions. As electrons have higher mobility compared to ions, this radiation loss is more important for electrons. The bremsstrahlung power density losses W_B with the relativistic corrections and the temperature anisotropy is given by [3]:

$$W_B\left[\frac{erg}{cm^3.s}\right] = 1.5\times 10^{-25} n_e$$

$$\sum_{k=1,2} n_k Z_k^{\,2}\left(B^{\frac{2}{3}}\, T_{\parallel}(eV)\right)^{\frac{1}{2}}\left(\frac{1 + 2\beta^{\frac{2}{3}}\, T_{\parallel}(eV)}{500{,}000}\right), \tag{14}$$

where Z_k is the charge number of particle k, n_e, and n_k are the electron density and the ion densities of particle k, respectively. The mechanical expansion power loss is estimated by [3]

$$W_m[\frac{erg}{cm^3.s}] = 1.02 \times 10^{18}[\beta^{\frac{2}{3}} T_{\parallel}(eV) + T_i(eV)]^{1.5}\left(\frac{\rho}{R}\right). \tag{15}$$

The ignition criteria are derived by explicitly writing follow equation

$$f_{\alpha} W_f - W_B - W_{he} - W_m \geq 0 \,. \tag{16}$$

The solution of the equality of the above equation describes a surface in the 3D space of ρR-T_e -T_i. The ignition criterion is solved for the general case where there is electron temperature anisotropy and ion temperatures are not equal to the electron temperature. We obtain a quadratic inequality in ρR as in the following:

$$Y_{DT} \equiv a(T_e,T_i)(\rho R)^2 + b(T_e,T_i)(\rho R) + c(T_e) \geq 0 \quad (17)$$

where

$$a(T_e,T_i) = 8.07\times10^{40} < \sigma v > -8.63\times10^{21} \quad (18)$$

$$\left(\beta^{\frac{2}{3}}T_{\parallel}(eV)\right)^{\frac{1}{2}} \times \left(1 + \frac{2\beta^{\frac{2}{3}}T_{\parallel}(eV)}{500{,}000}\right)$$

$$b(T_e,T_i) = -1.02\times10^{18}\left(\beta^{\frac{2}{3}}T_{\parallel}(eV) + T_i(eV)\right)^{1.5} \quad (19)$$

$$c(T_e) = -\frac{3.11\times10^{9}\left(\beta^{\frac{2}{3}}T_{\parallel}(eV)\right)^{\frac{7}{2}}}{\ln\Lambda}. \quad (20)$$

3.The ignition criterion

In the high-intensity laser, a shock wave is generated by the laser beam in the target material. This occurs when the intensity of the laser exceeds a certain threshold, typically exceeding 10^{21} w/cm^2. The shock wave is formed due to the rapid heating and compression of the target material by the intense laser pulse. Relativistic shock waves can also be generated in this regime. These shock waves occur when the velocity of the shock wave approaches the speed of light, resulting in relativistic effects such as changes in mass, energy, and momentum as observed from different reference frames. The presence of temperature anisotropy, where the ion and electron temperatures differ, further complicates the dynamics of the shock wave. The anisotropy is caused by the preferential heating of the plasma in the direction of the laser wave propagation. This anisotropy leads to different pressure gradients and energy transport mechanisms within the plasma. The plasma energy is given by:

$$E_{content} = \int (\frac{3}{2} n_i k_B T_i + \frac{3}{2} n_e k_B T_e) dV \quad . \quad (21)$$

So, the igniter performance can be analyzed by an energy balance which depends on the ion and electron temperature:

$$\left(\frac{3}{2}\right)\frac{d}{dt}\left(n_e k_B \beta^{\frac{2}{3}} T_{\parallel}\right) = \eta_d W_d + W_{ie} - W_B + f_a \eta_f W_f \quad (22)$$

$$\left(\frac{3}{2}\right)\frac{d}{dt}\left(n_i k_B T_i\right) = (1-\eta_d) W_d - W_{ie} + f_a (1-\eta_f) W_f \quad (23)$$

where k_B is Boltzmann's constant, W_d is the power density deposited by the driver, η_d is the fraction of the driver energy deposited in the electrons, W_{ie} is the ion-electron exchange power density, W_B is the electron bremsstrahlung power density losses, η_f is the energy fraction that is deposited in the electrons by the α-particles created in the fusion under consideration and (1- η_f) describes the energy fraction that is deposited in the ions by these alpha-particles and W_f is the fusion power density created in the shocked volume. Note that there are no heat waves and mechanical losses during the time when the shock wave is driven by the laser-piston. Consider the ion density for the content of DT plasma as $n_i = n_D + n_T$. For a neutral plasma with ionization Z_i, the electron density n_e is related to the ion density n_i by $\sum_{i=D,T} Z_i n_i$. In the fusion plasma, bremsstrahlung radiation causes electrons to have lower temperatures than ions. As a result of this temperature difference, there will be an ion-to-electron energy transfer. The ion electron exchange power density is given by [3]:

$$W_{ie}\left[\frac{erg}{cm^3.s}\right] = 2.70\times10^{-22} n_e \left(\frac{T_i(KeV) - \beta^{\frac{2}{3}}T_{\parallel}(KeV)}{\left(\beta^{\frac{2}{3}}T_{\parallel}(KeV)\right)^{1/5}}\right) \quad (24)$$

$$\sum_k \frac{Z_k{}^2 n_k}{m_k} \ln\Lambda_{ek}$$

where $\ln\Lambda_{ek}$ is the electron Coulomb logarithm term. The deposition power density W_d is dependent on the laser intensity I_L, pulse time duration τ_L and the shock compression $\kappa=\rho/\rho_0$,

$$W_d\left[\frac{erg}{cm^3.s}\right] = \frac{1}{4\times10^3}\frac{I_L\left(\frac{\omega}{cm^2}\right)\kappa}{\tau_L(s)} \quad (25)$$

The relation between the deposition power density and the laser parameters, as well as the particle u_p and shock u_s velocities, is obtained from the Hugoniot-Rankine equations. The fraction of the driver energy deposition into the electrons η_d can be estimated as [12]

$$\eta_d = \frac{\lambda_i}{\lambda_i + \lambda_e}, \quad (26)$$

where λ_i and λ_e are the appropriate mean free paths of the ions and electrons in plasma and are derived by the following

$$\lambda_i[cm] = \left(\frac{3\times10^{23}}{n_i}\right)\left(\frac{m_p}{m_i}\right)E_i[MeV], \quad (27)$$

$$\lambda_e[cm] = \left(\frac{\sqrt{\pi}Ze^3\times10^{23}}{3n_e^{3/2}\sqrt{k_B{}^3 T_{\perp}{}^2 T_{\parallel}}}\right)(\beta^{\frac{2}{3}}T_{\parallel}(KeV))^{\frac{3}{2}}E_i[MeV], \quad (28)$$

and

$$E_i = \frac{1}{2}m_i u_p{}^2 = 1250\,(MeV)\left(\frac{u_p}{c}\right)^2. \quad (29)$$

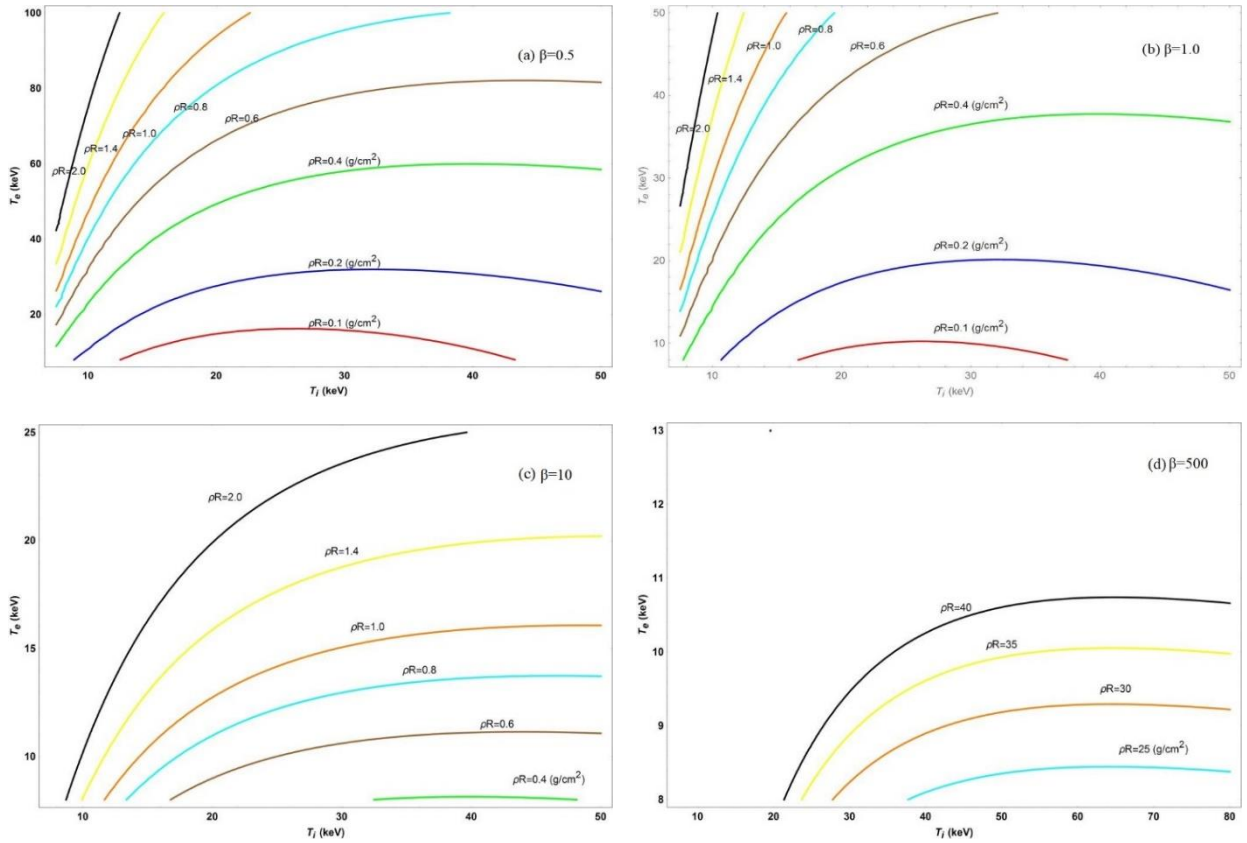

Figure 1. Contours of the confinement parameter ρR as a function of ions and electrons temperatures for the variant temperature anisotropy $\beta = T_{\perp}/T_{\parallel}$, (a) for β=0.5, (b) for β=1, (c) for β=10 and (d) for β=500.

Also, the energy fraction that is deposited in the electrons by the α-particles created in the fusion under consideration, η_f, is given by [12]:

$$\eta_f = \frac{32}{32 + \beta^{\frac{2}{3}} T_{\parallel}(keV)}. \qquad (30)$$

The time-dependent temperature equations are coupled to equations for the number densities of the ion species as

$$\frac{dn_D}{dt} = \frac{dn_T}{dt} = -\frac{dn_\alpha}{dt} = -n_D n_T \prec \sigma v \succ_{DT}, \qquad (31)$$

where n_D, n_T and n_α are the number densities of the deuterons, tritons, and, α-particles. In this paper, a laser intensity of 7.5×10^{22} w/cm^2, 1ps pulse duration, and energy of 3.67 kJ are considered. The fast ignition shock generated by irradiation can induce a compression of κ=4. The compression factor, denoted by κ=4, indicates the degree to which the target material is compressed [3]. A compression factor of 4 implies that the material has been compressed to one-fourth of its original volume.

4. Results and discussions

Contours of the confinement parameter ρR as a function of ion and electron temperatures are shown in figures 1(a), 1(b), 1(c), and 1(d) for different temperature anisotropy β. The results for figure 1 have been obtained using equation 17.

It is seen that in the absence of temperature anisotropy, β=1, for temperatures T_i, T_e in the range 10-50 keV, ρR<1. For the temperature anisotropy β=0.5, the confinement parameter ρR < 1 is obtained in return T_i, T_e in the range 10-50 keV. But for the temperature anisotropy β=10, the confinement parameter ρR < 1 is obtained in return T_e<15 keV and T_i> 12 keV. As the temperature anisotropy increases, the value of the confinement parameter increases. It is seen that the temperature ranges where ρR<40 are 20-80 keV for the ions and <10 keV for the electrons, for β=500. As shown in figures 1 (d), for the temperature anisotropy 500, the confinement parameter values, ρR, are higher compared to other figures. In general, acceptable surface densities are those that do not change the ion temperature with an increase in electron temperature. In figure 1 (d), for a surface density of 25 and a maximum electron temperature of 8.5 keV, the ion temperature is about 55 keV. However, with an increase in surface density to 30, the ion temperature at the maximum electron temperature of about 10 keV becomes approximately 65 keV. And then, with an increase in electron temperature, the ion temperature does not increase anymore. Therefore, the acceptable confinement parameter is 35, while in other figures, the confinement parameter value is less than this value. Moreover, the values of the confinement parameter are larger by about twenty orders of magnitude than for β=1, requiring larger pre-compression, igniter size, and larger energy laser. Figure 2 has been obtained using equations 22 and 23. As shown in figure 2 (a) and figure 2 (b), for deuterium-

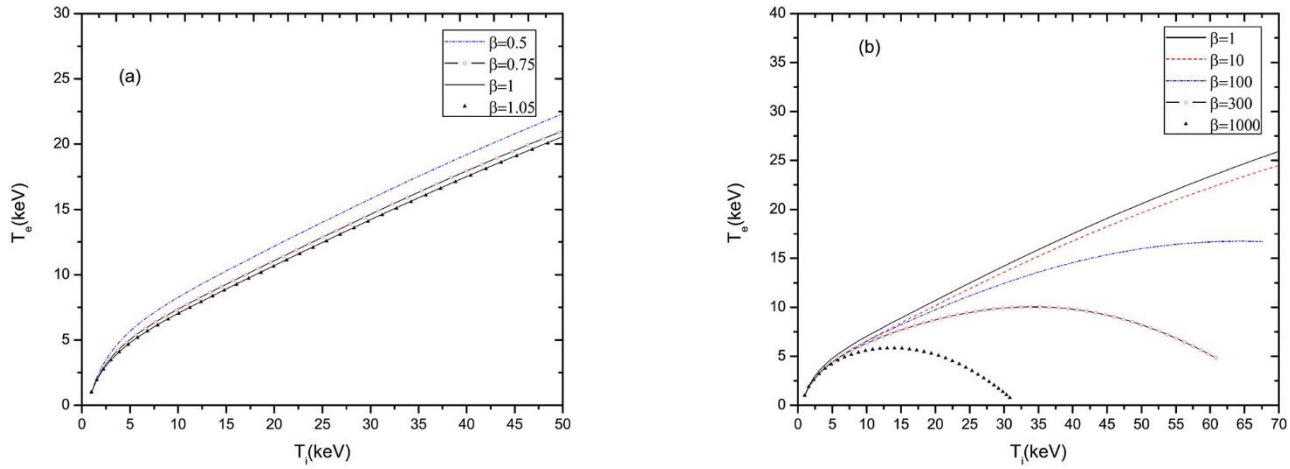

Figure 2. The confinement parameter curve in T_{e} and T_{i} plane for the variation value of the temperature anisotropy $\beta = T_{\perp}/T_{\parallel}$, (a) for $\beta \leq 1$ and (b) for $\beta \geq 1$.

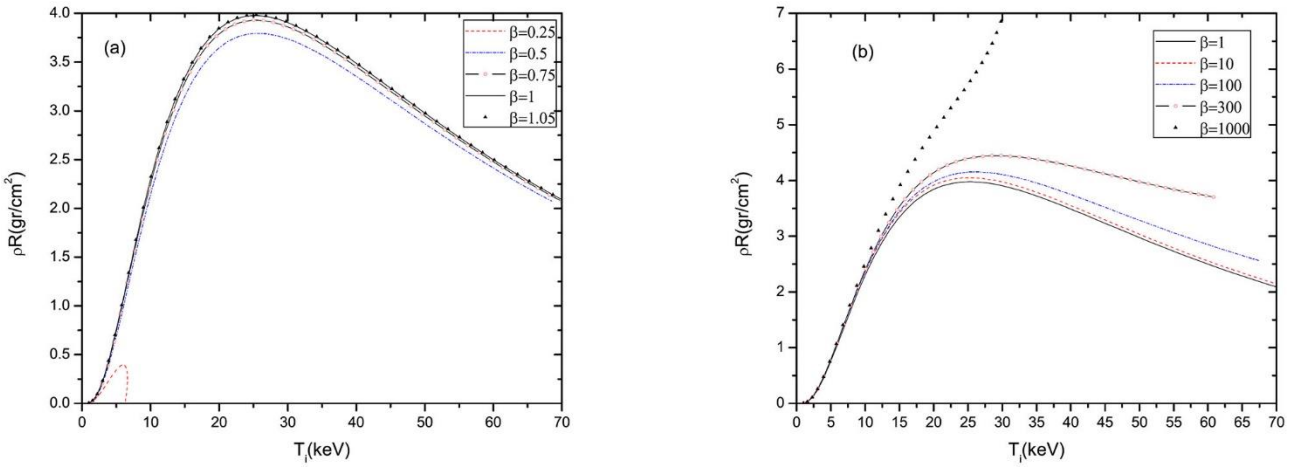

Figure 3. The confinement parameter, ρR, as a function of the ions temperatures for fixed the temperature anisotropy $\beta = T_{\perp}/T_{\parallel}$, (a) for $\beta \leq 1$ and (b) for $\beta \geq 1$.

tritium fuel pre-compressed to density n_0= 600 g/cm^3 and, a fixed confinement parameter, increasing the temperature anisotropy of the electron will reduce the temperature range of the electron. Figure 2 (b) shows that for temperature anisotropy β>100, we will achieve the same amount of confinement parameter with an electron temperature range of less than 20 keV. For temperature anisotropy β=300, we will find the electron temperature much smaller than 5 keV of this confinement parameter.

The confinement parameter first increases with increasing ion temperature and reaches its maximum value then decreases. As the temperature anisotropy increases, the maximum value of the confinement parameter increases. According to equation 17, for β= 0.25, the maximum confinement parameter is less than 0.5. See figure 3 (a). As it is shown in figure 3, For β<1, the maximum confinement parameter is less than 4. But for β>1, the maximum confinement parameter is more than 4. In times less than 1×10^{-13}s, the quadratic inequality equation (17) will not have a real physical answer for the product ρR. With increasing temperature, equation (17) has real solutions. According to equations (17), (22), and (23), the confinement parameter product as a function of time for the DT fuel that may reach ignition according to the criterion considered here is displayed in figure 4 (a) and figure 4 (b). When the ions and electrons temperatures are slightly higher than 10 keV and ignition is set on, the confinement parameter decreases to ρR=0.2 g/cm^2 at about 0.3 ps. Then the fusion energy deposition rises and exceeds the shock wave energy deposition.

With increasing temperature anisotropy per β<0.5, the confinement parameter will grow rapidly. With increasing temperature anisotropy per 300>β>0.5, the confinement parameter will increase slowly. See figure 5.a and figure 5.b. It is seen that the confinement parameter increases to about 4 gr/cm^2. At the end of the laser pulse, at 1ps, the confinement parameter reaches 4 gr/cm^2 and this value will increase with increasing temperature anisotropy.

For the different values of the temperature anisotropy, fusion energy density, W_f, radiation losses, W_b, deposition power density, W_d, and electron-ion exchange energy density, W_{ei}, as a function of time are given in figure 6 and figure 7. Figures 6 and 7 have been obtained using equations (2), (14), (24), (25), (22), and (23). The fraction of absorbed α-particles in the hot spot as a function of time for variation value of the temperature anisotropic is shown in figure 8. It is seen that as time evolves and the temperatures increase, a larger fraction of α-particles leaves the igniter region heating up the surroundings. For $\beta = T_{\perp}/T_{\parallel}$<1, the fusion energy fraction

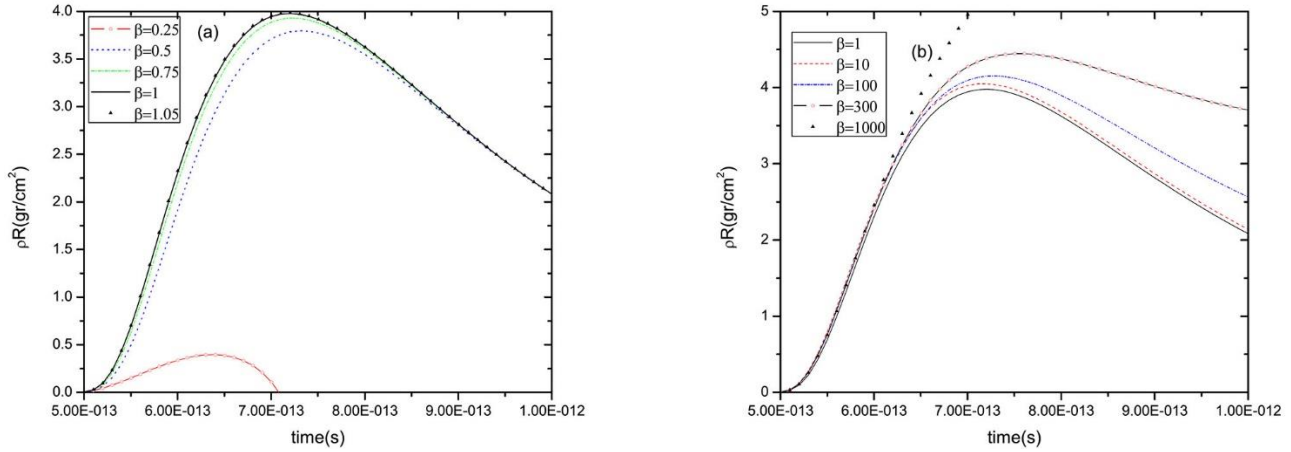

Figure 4. The confinement parameter, ρR, as a function of time for fixed the temperature anisotropy $\beta = T_{\perp}/T_{\parallel}$, (a) for $\beta \leq 1$ and (b) for $\beta \geq 1$.

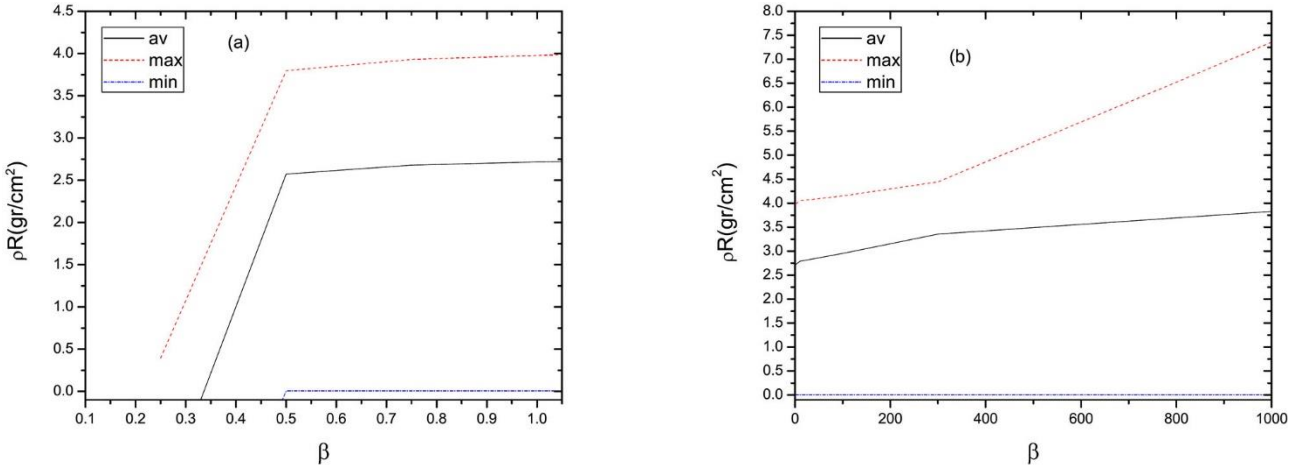

Figure 5. The confinement parameter changes in terms of the temperature anisotropy $\beta = T_{\perp}/T_{\parallel}$, (a) for $\beta \leq 1$ and (b) for $\beta \geq 1$.

deposited, f_{α}, decreases with time and at the end of the laser pulse i.e. t=1ps reaches its minimum value of about 0.1. Figure 8 has been obtained using equations (9), (10), (11), and (12). So by reducing the anisotropy parameter, β, this minimum value will be less than 0.1. For $\beta = T_{\perp}/T_{\parallel} > 300$, f_{α} first decreases with increasing time and reaches its minimum value. Then fusion energy fraction deposited, f_{α}, increases with time. Figure 9 has been obtained using equations (9), (10), (11), and (12). As shown in figure 9 .a and Fgure 9 .b, the maximum constant energy fraction will be about 0.9. For a maximum of $\beta > 200$, the deduction will increase. For $\beta = 1000$, the energy fraction value will reach 0.92. At the end of the laser pulse, the minimum fusion energy fraction per $\beta < 1$ will be in the range of 0.085-0.05. The fusion energy fraction, f_{α}, will increase as the temperature anisotropy parameter increases.

5. Conclusions

This paper has investigated the impact of temperature anisotropy on the fuel ignition criterion for DT pre-compressed plasma. The temperature anisotropy can have several implications on the ignition condition for deuterium-tritium fuel. The temperature anisotropy can affect the minimum conditions required for achieving ignition in DT fuel. The presence of anisotropy may change the critical values of temperature, density, and confinement time necessary for sustained fusion reactions. The efficiency of ignition, which is defined as the ratio of fusion energy output to the input energy, can be influenced by temperature anisotropy. Anisotropic conditions may affect the energy deposition of beams in the fuel plasma, leading to variations in the energy transfer efficiency and, consequently, the overall ignition efficiency. Temperature anisotropy can impact the stability of the ignition process. Anisotropic conditions may introduce instabilities and fluctuations in the plasma, which can affect the confinement and energy transfer mechanisms. These instabilities can hinder the sustained ignition of the fusion reactions. Anisotropic temperature distributions can lead to increased energy loss and dissipation within the plasma. The presence of temperature gradients and anisotropy can enhance radiative losses and cause energy to be transferred to other plasma particles via various mechanisms, reducing the available energy for fusion reactions and potentially affecting the ignition conditions. Temperature anisotropy can influence the interactions between the injected beams

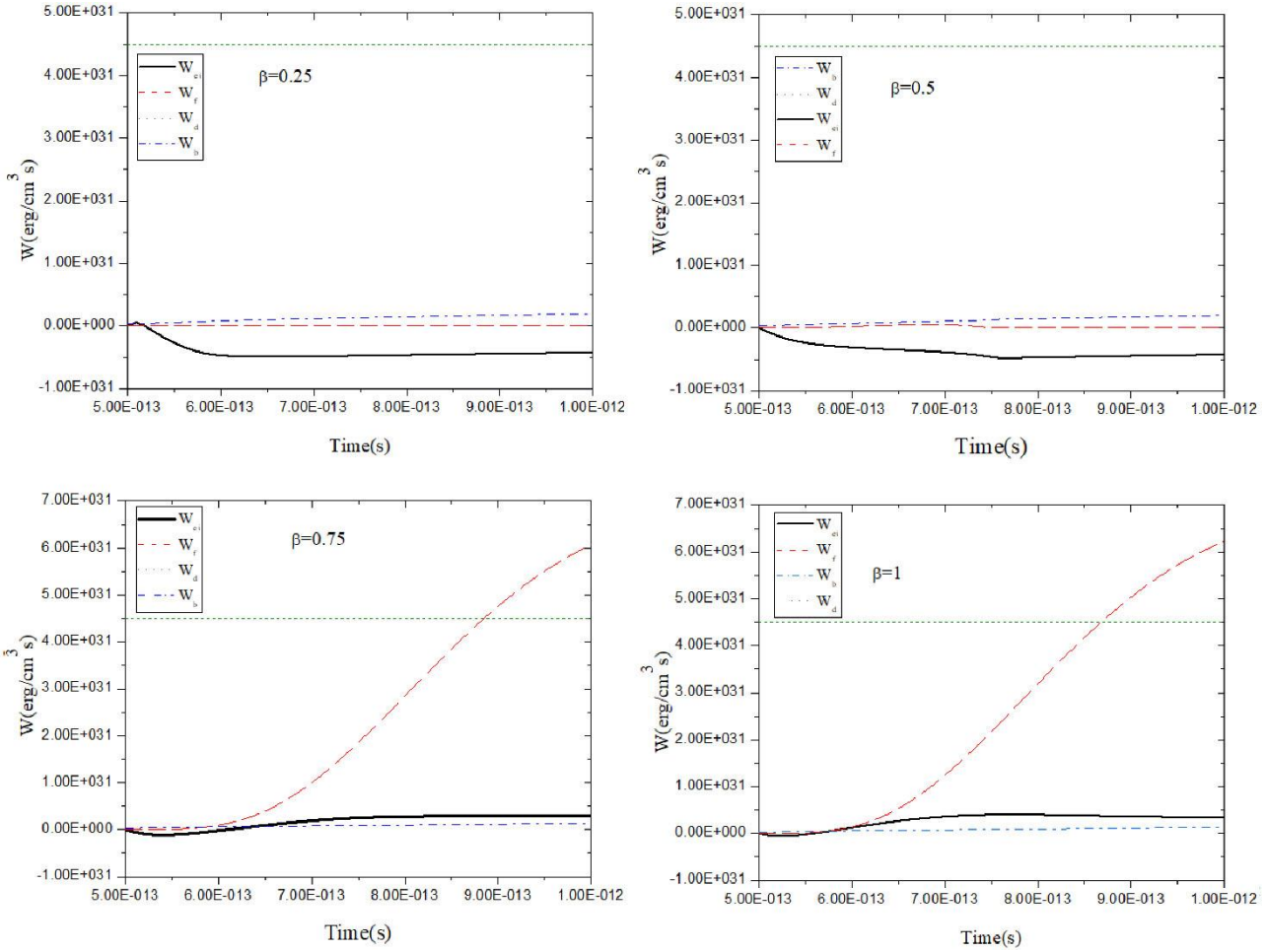

Figure 6. Various energy power density terms as a function of time for the DT fuel for the variation value of the temperature anisotropic, $\beta = T_{\perp}/T_{\parallel} \leq 1$.

and the fuel plasma. Anisotropic conditions can affect the beam propagation, scattering, and energy deposition processes, altering the heating and compression dynamics required for ignition. The paper "Introducing a two temperature plasma ignition in inertial confined targets under the effect of relativistic shock waves" by Eliezer et al. suggests using a two-temperature laser-induced shock wave in the intermediate domain between relativistic and non-relativistic shock waves, without mentioning the dependence of temperature anisotropy. In contrast, our paper investigates the influence of temperature anisotropy on the ignition criterion of deuterium-tritium fuel in fast ignition fusion schemes. It explores the impact of increasing the temperature anisotropy parameter on the fraction of alpha particles created and deposited into the ignition domain, as well as the fusion energy fraction throughout the laser pulse irradiation of the fuel.

In this paper, picosecond laser pulses interact with the deuterium-tritium fuel to generate a fast electron beam that reaches the pellet core and ignites the fuel. The ignition criterion is determined by balancing fusion energy with expansion, radiation, and heat conduction losses, which depend on the electron temperature and temperature anisotropy. Temperature anisotropy has the greatest effect on fusion energy density and electron-ion exchange energy density. For $T_{\perp} < T_{\parallel}$, increasing the temperature anisotropy leads to an increase in fusion energy density, while for $T_{\perp} > T_{\parallel}$, it leads to a decrease in fusion energy density. When the anisotropy increases by a factor of 3 for $\beta > 1$, the electron-ion exchange energy density increases by 3.7 times, and the fusion energy density decreases by 1.1 times. The ignition criterion is described by a surface of electron and ion temperatures T_e, T_i, and confinement parameter ρR.

In the presence of temperature anisotropy $\beta = T_{\perp}/T_{\parallel} > 1$, DT fuel fusion requires higher temperatures to reach ignition compared to state $\beta = T_{\perp}/T_{\parallel} < 1$, mainly due to higher radiation losses, which implies larger size and more dense igniters. The value of plasma density times hot spot dimension required for DT fuel ignition for $\beta = 1000$ is larger by a factor of 1.88 or more than for $\beta = 1$. The fusion energy fraction f_{α} decreases during laser pulse irradiation of the fuel. However, during the interaction of picosecond laser pulses with the fuel pellet, increasing temperature anisotropy due to shock wave and sidebands coupling with the electron oscillatory velocity leads to an increasing fusion energy fraction.

In conclusion, the presence of temperature anisotropy in the fuel plasma can have significant implications for the ignition condition of D-T fuel, affecting the required

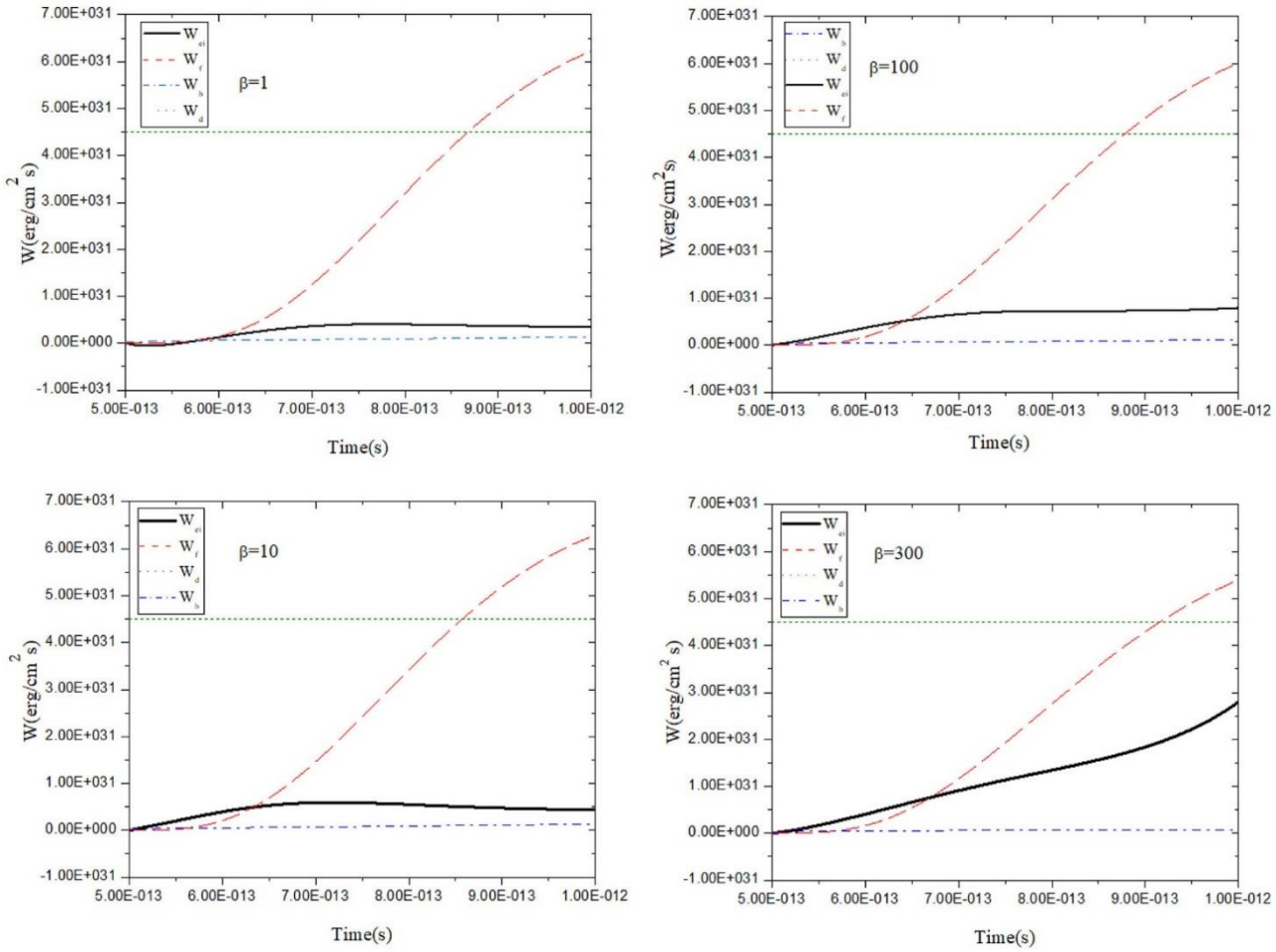

Figure 7. Various energy power density terms as a function of time for the DT fuel for variation value of the temperature anisotropic, $\beta = T_{\perp}/T_{\parallel} \geq 1$.

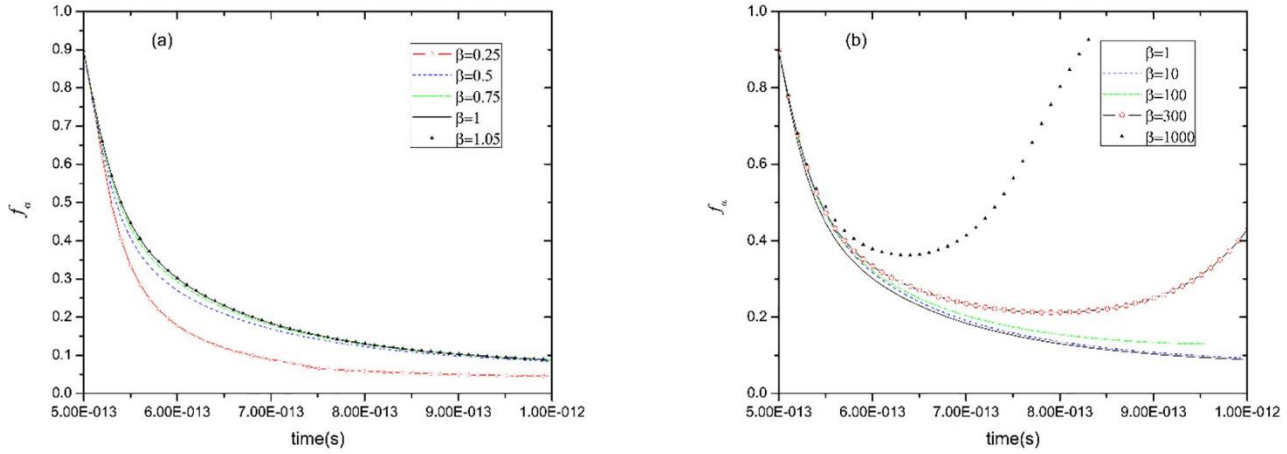

Figure 8. The fusion energy fraction deposited in the igniter domain for the DT fuel, f_{α}, as a function of the time for variation value of the temperature anisotropic,β, (a) for $\beta \leq 1$ and (b) for $\beta \geq 1$.

temperatures, ignition efficiency, stability, energy loss, and beam-plasma interactions. Further research is necessary to fully understand and quantify these implications and their impact on practical fusion systems.

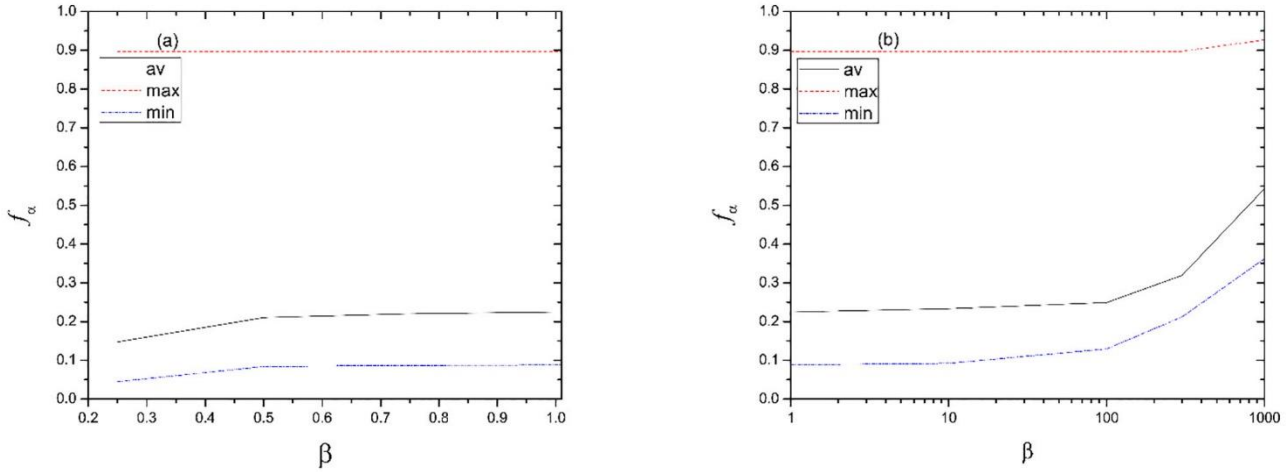

Figure 9. The fusion energy fraction changes as a function of the temperature anisotropy $\beta = T_\perp/T_\parallel$, (a) for $\beta \leq 1$ and (b) for $\beta \geq 1$.

References

1. A A Harms, K F Schoepf, and D R Kingdon, "Principles of fusion energy: an introduction to fusion energy for students of science and engineering", World Scientific (2000),.
2. M Temporal, B Canaud, V Brandon, and R Ramis, *Eur. Phys. J. D* **73** (2019) 1.
3. S Eliezer, Z Henis, N Nissim, S V Pinhasi, and J M M Val, *Laser and Particle Beams* **33** (2015) 577.
4. S S Razavipour and B Malekynia, *Indian J. Phys.* **87** (2013) 1109.
5. O Kamboj, H S Ghotra, V Thakur, J Pasley, and N Kant, *The European Physical Journal Plus* **136** (2021) 1.
6. M Tabak, J Hammer, M E Glinsky, W L Kruer, S C Wilks, J Woodworth, E M Campbell, M D Perry, and R J Mason, *Physics of Plasmas* **1** (1994) 1626 .
7. D X Liu, W Hong, L Q Shan, S C Wu, and Y Q Gu, *Plasma Physics and Controlled Fusion* **53** (2011) 035022.
8. M Temporal, B Canaud, W Cayzac, and R Ramis, *Eur. Phys. J. D* **75** (2021) 1.
9. S Pfalzner, "An introduction to inertial confinement fusion", CRC Press (2006).
10. M Mahdavi and F Khodadadi Azadboni, *Journal of Fusion Energy* **31** (2012) 396.
11. V A Burtsev, S Yu Gus' kov, V B Rozanov, D V Il'In, A A Levkovsky, V E Sherman, Yu N Starbunov, and N V Zmitrenko., *Laser and Part. Beams* **11** (1993) 669.
12. S Atzeni and J Meyer-ter-Vehn, "The physics of inertial fusion: beam plasma interaction, hydrodynamics, hot dense matter" OUP Oxford, Vol. 125 (2004).
13. E S Weibel, *Physical Review Letters* **2** (1959) 83.
14. M Mahdavi and F Khodadadi Azadboni, *Journal of Fusion Energy* **35** (2016) 154.
15. L A Cottrill, A B Langdon, B F Lasinski, S M Lund, K Molvig, M Tabak, R P J Town, and E A Williams, *Physical Review E* **15** , 3 (2008) 082108 .
16. K M Schoeffler, L O Silva, *Physical Review Research* **2** (2020) 033233.
17. C Davidson, Z M Sheng, T Wilson, and P McKenna, *Journal of Plasma Physics* **88** (2022) 1.
18. C Zhang, J Hua, Y Wu, Y Fang, Y Ma, T Zhang, and C Joshi, *Physical Review Letters* **125** (2020) 255001.
19. Pokhotelov, Oleg A, et al., *Journal of Geophysical Research: Space Physics* **107**.A10 (2002): SMP-18.
20. R Fitzpatrick, "*Plasma physics: an introduction*", CRC Press (2022).
21. M Mahdavi, and F Khodadadi Azadboni, *Physics of Plasmas* **20** (2013) 122708.
22. M Takamoto, Y Matsumoto, and T N Kato, *The Astrophysical Journal Letters* **860** (2018) L1.
23. T Jikei and T Amano, *Physics of Plasmas* **29** (2022) 022102.
24. R F Post, *Fusion technology* **35** (1999) 40.
25. L Nicolas, "Effects of collisions on the magnetic streaming instability"; Doctoral dissertation, Paris (2017).
26. M Iwamoto, T Amano, M Hoshino, and Y Matsumoto, *The Astrophysical Journal* **858** (2018) 93.
27. A Sid, A Ghezal, A Soudani, and M Bekhouche, *Plasma and Fusion Research* **5** (2010) 007.
28. A Bret, *The Astrophysical Journal* **699** (2009) 990.
29. F B Marcus, "*Inertial Fusion and Magnetic Fast Pulsed Systems*" Systems Approaches to Nuclear Fusion Reactors. Cham: Springer International Publishing, (2023).
30. R Jung, "*Laser-plasma interaction with ultra-short laser pulses*" VDM-Verlag Dr. M ller (2008).
31. B Du, H B Cai, W S Zhang, J M Tian, E H Zhang, S Y Zou, and S P Zhu, *Plasma Physics and Controlled Fusion* **62** (2019) 025017.